Mycopathologia (2025) 190:42
https://doi.org/10.1007/s11046-025-00949-3

ORIGINAL ARTICLE

Transcriptomics Uncovers Key Genes for Photodynamic Killing on *Trichosporon asahii* Biofilms

Wanting Luo · Guoliang Wang · Hongyu Chang · Guiming Liu · He Zhu · Haitao Li

Received: 22 December 2024 / Accepted: 18 April 2025

Abstract

Background The escalating threat of antifungal resistance stemming from *Trichosporon asahii* (*T. asahii*) biofilms necessitates the pursuit of innovative therapeutic strategies. Among these approaches, 5-aminolevulinic acid (ALA) photodynamic therapy (PDT), an emerging therapeutic modality, has exhibited promising potential in eradicating *T. asahii* biofilms.

Methods The inhibitory activity was evaluated by confocal laser scanning microscopy. To delve deeper into the efficacy of ALA-PDT in eliminating *T. asahii* biofilms, we conducted a comprehensive transcriptional analysis utilizing transcriptome sequencing.

Results ALA-PDT demonstrated a profound inhibitory effect on the viability of *T. asahii* biofilms. Our investigation unveiled 2720 differentially expressed genes following exposure to ALA-PDT. Subsequent meticulous scrutiny allowed for the annotation of genes with a ≥ twofold change in transcription, focusing on Gene Ontology and Kyoto Encyclopedia of Genes and Genomes pathways. Particularly noteworthy were the upregulated genes associated

Wanting Luo, Guoliang Wang and Hongyu Chang have contributed equally to this work.

Handling Editor: Vishnu Chaturvedi

Supplementary Information The online version contains supplementary material available at https://doi.org/10.1007/s11046-025-00949-3.

W. Luo · H. Zhu (✉) · H. Li (✉)
Department of Dermatology, The Seventh Medical Center of PLA General Hospital, No.5 Nanmencang, Dongcheng District, Beijing 100700, China
e-mail: 137202744@qq.com

H. Li
e-mail: lihaitao_1976@sina.com

W. Luo
e-mail: 454628880@qq.com

W. Luo
Department of Dermatology, Shenzhen People's Hospital (The Second Clinical Medical College, Jinan University, The First Affiliated Hospital, Southern University of Science and Technology), No. 1017, Dongmen North Rd, Luohu District, Shenzhen 518020, China

G. Wang · G. Liu
Beijing Key Laboratory of Agricultural Genetic Resources and Biotechnology, Institute of Biotechnology, Beijing Academy of Agriculture and Forestry Sciences, No.11, Shuguang Huayuan Middle Road, Haidian District, Beijing 100097, China
e-mail: wangglpro@163.com

G. Liu
e-mail: mingguiliu@aliyun.com

H. Chang
Department of Pediatrics, the People's Liberation Army Rocket Force Characteristic Medical Center, No.6 Xinjijiekou Ouwai Street, Xicheng District, Beijing 100088, China
e-mail: chhyu_ep@126.com

Published online: 18 May 2025

with oxidation–reduction processes, oxidoreductase activity, and catalytic activity. Conversely, the downregulated genes were linked to ATP binding, protein phosphorylation, and protein kinase activity. Additionally, we observed a surge in the transcription of genes that may be involved in oxidative stress (e.g., A1Q1_05494) as well as genes that may be involved in morphogenesis and biofilm formation (e.g., A1Q1_04029, A1Q1_01345, A1Q1_08069, and A1Q1_01456) following ALA-PDT treatment.

Conclusions Our findings underscore the substantial impact of ALA-PDT on the transcriptional regulation of genes related to oxidative stress, morphogenesis, and biofilm formation, paving the way for novel therapeutic avenues in combating *T. asahii* biofilms.

Keywords Photodynamic therapy (PDT) · 5-aminolevulinic acid (ALA) · *Trichosporon asahii* (*T. asahii*) · Biofilm

Introduction

Trichosporon, an opportunistic genus of pathogenic fungi, has been identified in various natural environments, as well as on human skin and in tracts [1]. Clinically, there are over 50 recognized species of Trichosporon, out of which 16 have been implicated in human infections [1, 2]. Among these species, *Trichosporon asahii* (*T. asahii*) stands out as a leading cause of invasive infections [3, 4]. Transmission of the fungus can occur through the skin, tracts, or invasive medical devices, resulting in trichosporosis, which manifests as superficial fungal disease, summer-type hypersensitivity pneumonitis, and other invasive infections [1, 5, 6]. *T. asahii* infections are particularly associated with high mortality rates in immunocompromised patients, including those with neutropenia or hematological disorders undergoing chemotherapy, organ transplant recipients, advanced cancer patients, or individuals with AIDS [7–9]. Moreover, disseminated *T. asahii* infections have also been reported in immunocompetent patients [10, 11]. Notably, the incidence of invasive trichosporosis is accompanied by an alarmingly high overall mortality rate of 68.7% [3]. Critically ill COVID-19 patients with *T. asahii* fungemia have reported a staggering 30-day mortality rate as high as 80% [12].

Previous investigations have provided substantial evidence regarding the capacity of *T. asahii* to form biofilms that exhibit remarkable resistance to a wide range of commonly prescribed first-line antifungal agents [13]. *T. asahii* biofilm drug resistance remains an imposing problem that necessitates innovative approaches for resolution [14, 15].

Photodynamic therapy (PDT) has emerged as a promising antifungal treatment, particularly for mucocutaneous infections [16]. PDT has been shown to overcome traditional resistance mechanisms, leading to a decreased incidence of drug resistance development [17]. PDT involves the utilization of a photosensitizer (PS) along with light source irradiation, triggering a cascade of reactions that generate a substantial amount of harmful radicals, including reactive oxygen species (ROS) and reactive nitrogen species (RNS), capable of inflicting irreversible damage to cells [18, 19]. Although the ability of light-drug combinations to eradicate microorganisms has been recognized for over a century, in-depth investigations into this phenomenon have gained momentum only recently, driven by the search for alternative treatments against antibiotic-resistant pathogens [20]. PDT exhibits a remarkable predilection for targeting fungal cells over human cells, and there have been no reported instances of fungal resistance or associations with genotoxic or mutagenic effects, underscoring its favorable safety profile as a therapeutic modality [20].

In recent years, encouraging outcomes have been reported in the treatment of superficial skin fungal infections [5, 21, 22], including the utilization of 5-aminolevulinic acid (ALA) PDT for skin infections caused by *T. asahii* [5]. However, the underlying mechanisms of PDT in treating fungal infections remain largely unexplored. The present study aims to evaluate the efficacy of PDT on *T. asahii* biofilms in vitro and elucidate its underlying mechanism of action.

Materials and Methods

Preparation of T. asahii Biofilm

The *T. asahii* isolate 06108 was employed in this investigation due to its high biofilm production. The isolate was derived from the nail of a Chinese patient in Qilu Hospital and kindly offered by Peking

University First Hospital. Strain identification was conducted by sequencing the IGS1 region. The tested strain was passage cultured on Potato Dextrose Agar (PDA, Hopebio, Qingdao, China) at 35 ℃ to ensure their optimal vitality through passage cultivation. Single colonies were collected and overnight cultures of *T. asahii* were prepared in yeast-extract peptone dextrose medium. After centrifugation and double washing with Phosphate Buffered Saline (PBS, Leagene, Beijing, China), the cultures were resuspended in fresh RPMI 1640 medium (Sigma-Aldrich) at a concentration of $(1–2)\times10^6$ CFU/ml for subsequent biofilm formation. The *T. asahii* suspensions, at the mentioned concentration, were pipetted into 24-well polystyrene plates and adhesion for 6 h at 35 ℃. Following gentle washing with PBS to remove nonadherent cells, RPMI-1640 medium was replenished in each well, with subsequent daily replacement to maintain optimal biofilm development conditions. After adhesion, *T. asahii* cells were incubated at 35 ℃ for 48 h for biofilm formation. Mature biofilms formed in the plates were gently washed with PBS to eliminate planktonic cells prior to subsequent experiments.

Photosensitizer and Light Source

A stock solution of 5-aminolevulinic acid hydrochloride (ALA, Fudan Zhangjiang Bio-Pharm, Shanghai, China) at a concentration of 150 mM was prepared by dissolving it in 0.9% NaCl. The solution was then filter-sterilized and carefully stored in the dark at 4 ℃ to maintain its stability. The photosensitizer solution was incubated with *T. asahii* biofilms in the dark for 3 h. The LED-IB photodynamic therapy instrument (Yage Optic and Electronic Technique Co., Ltd., Wuhan, China) emitting light at a wavelength of 635 nm was administered in the experiment. The fluence rate of 80 mW/cm^2 was set and the light intensities of 0, 100, 200 J/cm^2 were used. The concentration of ALA (150 mM) and light irradiation parameters were selected based on a previous study[5].

This experimental groups were divided as follows.

Group P^-L^-: the prewashed mature biofilms were incubated with 0.9% NaCl without photosensitizer and irradiation of red light.

Group P^-L^{100}: the prewashed mature biofilms were incubated with 0.9% NaCl and then irradiated at 80 mW/cm^2 for 21 min (light intensity of 100 J/cm^2).

Group P^-L^{200}: the prewashed mature biofilms were incubated with 0.9% NaCl and then irradiated at 80 mW/cm^2 for 42 min (light intensity of 200 J/cm^2).

Group P^+L^-: the prewashed mature biofilms were incubated with ALA at a concentration of 150 mM in the dark for 3 h without irradiation of red light.

Group P^+L^{100}: the prewashed mature biofilms were incubated with ALA at a concentration of 150 mM in the dark for 3 h and then irradiated at 80 mW/cm^2 for 21 min (light intensity of 100 J/cm^2).

Group P^+L^{200}: the prewashed mature biofilms were incubated with ALA at a concentration of 150 mM in the dark for 3 h and then irradiated at 80mW/cm^2 for 42 min (light intensity of 200 J/cm^2).

CLSM and Viability

The effect of ALA-PDT on the structure and viability of *T. asahii* was evaluated using CLSM. Biofilms were stained by LIVE/DEAD BacLight bacterial viability kit (Thermo Fisher Scientific, USA) at room temperature in the absence of light following the manufacturer's protocol. This kit, containing propidium iodide (PI) and STYO9, was employed to assess the viability of cells within the biofilm and determine the number of viable and dead cells. Stained biofilms were visualized using a TCS-SP8 confocal laser scanning microscope (Leica, Germany), with images captured from three randomly chosen locations per sample. Subsequently, Leica confocal software was utilized to analyze the ratio of red and green fluorescence, enabling quantification of the inhibitory effect. The inhibition rate was calculated as [Dead/(Live + Dead)]*100%. The results are reported as the mean ± SD and processed with SPSS Statistics 24.0 software. The differences among groups were tested using a One-way Analysis of Variance (ANOVA).The post hoc Tamhane's test was used for the comparison between groups due to unequal group variances. The level of significance was set at $p < 0.05$.

RNA Extraction, Library Construction and Sequencing

Total RNA was extracted from *T. asahii* biofilms of six groups, with three biological replicates performed. Briefly, *T. asahii* biofilm cells were harvested, washed with PBS, and stored at − 80℃ until further use. Total RNA samples were prepared from freeze-dried cells

using the Ultrapure RNA kit (Cat.CW0581M, Cowin Bio.) following the manufacturer's instructions, and mRNA was enriched using VAHTS mRNA Capture Beads (Cat.N401). The The concentration and quality of RNA was measured using Qubit 3 Fluorometer and gel electrophoresis. For global transcriptome analysis, high-throughput mRNA sequencing (RNA-Seq) was conducted. RNA-Seq libraries were generated from mRNA using the VAHTS Universal V8 RNA-seq Library Prep Kit and then sequenced on the Illumina NovaSeq 6000 platform.

Sequencing Data and DEG Analysis

Quality of fastq files was assessed with FastQC. Adapters and low-quality segments were trimmed with Trimmomatic. Filtered reads were aligned to the *Trichosporon asahii* var. *asahii* CBS 2479 genome using Hisat2 [23–25] and the count matrix was generated using featureCounts. All subsequent gene expression data analyses were carried out in the *R* software. Differential gene expression analysis between different groups was performed using DESeq2 package [26], with FDR < 0.05 and $|\log_2 (\text{fold change})| \geq 2$. The identified DEGs were subjected to GO and KEGG enrichment analyses. The sequence data reported in this paper have been deposited in the Genome Sequence Archive [27] in National Genomics Data Center [28], China National Center for Bioinformation/Beijing Institute of Genomics, Chinese Academy of Sciences (with accession number PRJCA015533, accessible at https://ngdc.cncb.ac.cn/). And the RNA-seq data was also submitted to NCBI Sequence Read Archive (accession number SRP458245) and BioProject (accession number PRJNA1012498).

qRT-PCR Validation

Selected DEGs were verified by qRT-PCR. First strand cDNA synthesis was performed using a reverse transcription kit (Vazyme, R312). The qRT-PCR analysis was conducted in triplicate with ACTIN (GenBank number XM_014323626) as a reference gene. The reaction system contained 10 µL of 2 × AceQ Universal SYBR qPCR Master Mix, 0.4 µL forward and reverse primers, and 2 µL of cDNA template for a total volume of 20 µL. The $2^{\wedge -\Delta\Delta Ct}$ expression level calculations were performed and were expressed as the mean ± SD derived from three independent measurements. Statistical significance of the values was determined using the Student's *t*-test, with a significance threshold of $p < 0.05$. The target genes, namely A1Q1_04029, A1Q1_08069, A1Q1_02782, A1Q1_05711, A1Q1_01345, A1Q1_01456 and A1Q1_05494, were amplified accordingly, and their primer sequences were listed in Table S1.

Results

ALA-PDT Suppresses Viability of T. asahii Biofilm

Utilizing confocal laser scanning microscopy (CLSM), we investigated the impact of ALA-PDT on the viability of *T. asahii* biofilm. Green fluorescence staining, achieved through the application of SYTO 9, which permeates all yeast membranes, facilitated the observation of the cells. Conversely, PI selectively penetrated yeasts with compromised membranes, leading to red fluorescence staining. CLSM images provided valuable insights into the viability of *T. asahii* biofilms under different intervention conditions. Notably, mature *T. asahii* biofilms treated with ALA-PDT exhibited a significant increase in red fluorescing cells compared to group P^-L^- (Fig. 1a). This increase was particularly prominent in group P^+L^{100} (Fig. 1e) and group P^+L^{200} (Fig. 1f), indicating considerable fungal cell damage. Group P^+L^{200}, exposed to higher light intensity, demonstrated a stronger red fluorescence intensity than group P^+L^{100}, highlighting a dose-dependent relationship with the applied light intensity. In contrast, group P^-L^- (Fig. 1a), group P^+L^- (Fig. 1d), group P^-L^{100} (Fig. 1b) and group P^-L^{200} (Fig. 1c) exhibited exclusively green fluorescent live cells.

To quantify cell viability, we analyzed the red/green fluorescence ratio (Dead/live ratio) of each biofilm image using Leica confocal software and calculated the inhibition rate accordingly (Table 1). Impressively, group P^+L^{200}, which received a light dose of 200 J/cm^2, achieved a remarkable inhibition rate of 75.58%. Statistical analysis (Fig. 2) confirmed the significant differences between the ALA-PDT treatment groups and the untreated control group. However, no statistically significant differences were observed among the untreated control group, group P^+L^-, group P^-L^{100} and group P^-L^{200}.

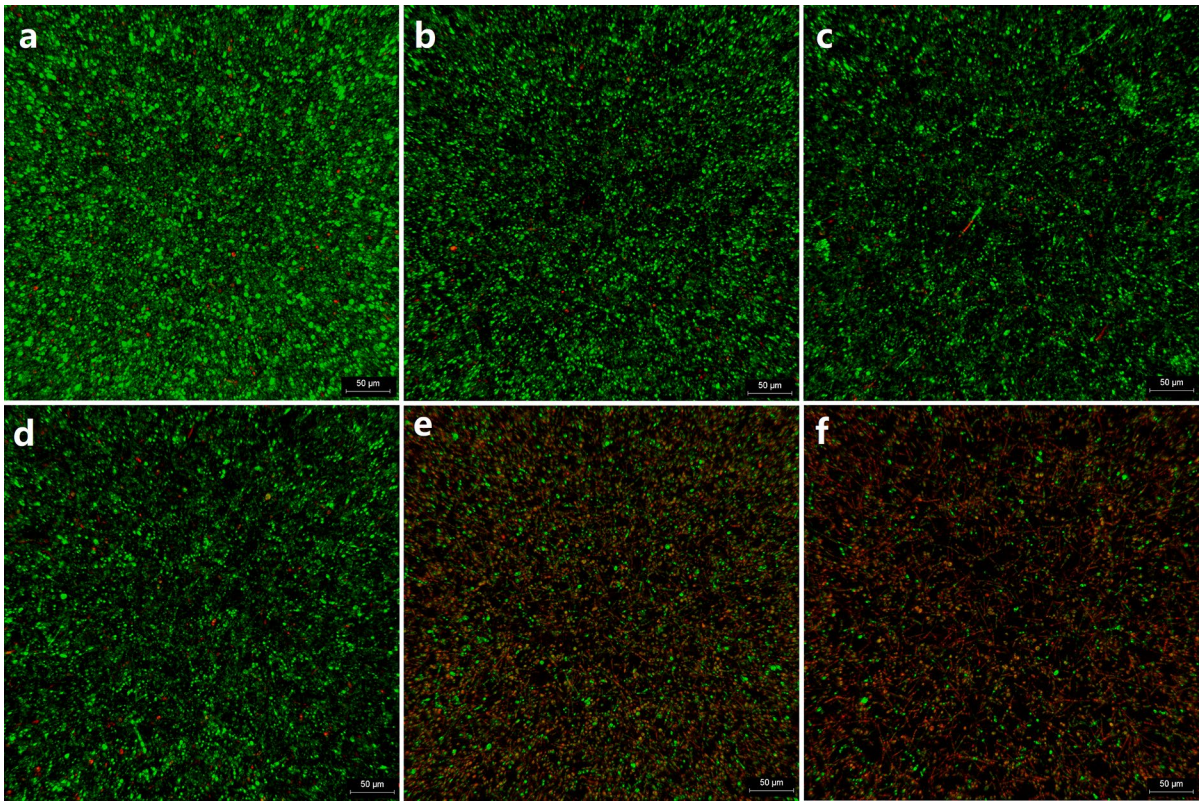

Fig. 1 Confocal laser scanning microscopy (CLSM) was employed to visualize *T. asahii* biofilm specimens under various ALA-PDT conditions. Live cells were green and dead cells were red. **a** group $P^{-}L^{-}$ (untreated control group); **b** group $P^{-}L^{100}$; **c** group $P^{-}L^{200}$; **d** group $P^{+}L^{-}$; **e** group $P^{+}L^{100}$; **f** group $P^{+}L^{200}$

Table 1 Inhibition effect of *T. asahii* biofilms on Dead/live ratio

Groups	ALA (mM)	Light (J/cm^2)	Inhibition rate
$P^{-}L^{-}$	0	0	0.14%
$P^{-}L^{100}$	0	100	0.27%
$P^{-}L^{200}$	0	200	0.54%
$P^{+}L^{-}$	150	0	1.84%
$P^{+}L^{100}$	150	100	46.20%
$P^{+}L^{200}$	150	200	75.58%

Transcriptome Sequencing and Analysis

For comprehensive transcriptomic analysis, we generated 18 RNA-sequencing (RNA-seq) libraries representing six distinct groups of *T. asahii* samples. Rigorous quality control procedures yielded a staggering 105.63 billion high-quality clean nucleotides. These reads were subsequently aligned to the

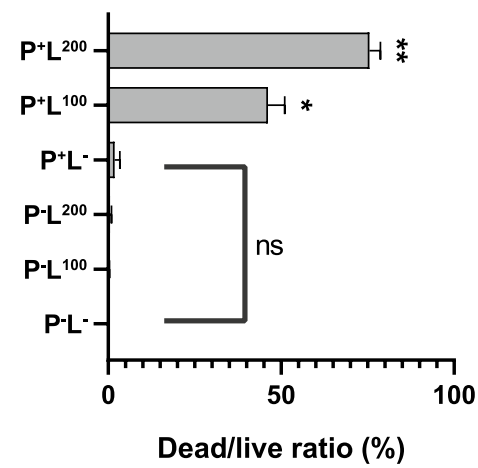

Fig. 2 Dead/live Ratio of *T. asahii* Biofilms Following ALA-PDT Exposure. Significant Differences Observed Between ALA-PDT Groups (group $P^{+}L^{100}$ and group $P^{+}L^{200}$) and untreated control group (*$p<0.05$, **$p<0.01$). No statistically significant differences between the control group, the ALA group (group $P^{+}L^{-}$), and the light group (group $P^{-}L^{100}$,_group $P^{-}L^{200}$)

reference genome, resulting in an average mapping rate of 74.23% for the high-quality clean reads. The excellent reproducibility of the RNA-seq data was confirmed by high Pearson correlation coefficients among the three biological replicates (ranging from 0.963 to 0.999, as shown in Table S2), underscoring the robustness and reliability of our study.

Differentially Expressed Genes (DEGs)

Pairwise comparisons were conducted to assess transcriptional disparities between different groups, focusing on genes exhibiting a fold change ≥ 2 and a false discovery rate (FDR) < 0.05. Notably, our analysis revealed a substantial number of DEGs in these comparisons. To examine the impact of ALA-PDT on *T. asahii* biofilms at the gene level, we compared DEGs between the untreated control group (group $P^{-}L^{-}$) and the ALA-PDT group (group $P^{+}L^{100}$ or group $P^{+}L^{200}$). Due to the similarity in gene expression between group $P^{+}L^{100}$ and group $P^{+}L^{200}$, subsequent analysis exclusively focused on the differential gene comparison between group $P^{-}L^{-}$ and group $P^{+}L^{100}$ (Fig. 3, FigS1, FigS2). This comparison identified a total of 2,720 DEGs, with 1,393 upregulated genes and 1327 downregulated genes in the group $P^{+}L^{100}$ compared to the untreated control group (Fig. 3 and Fig. 4a). Hierarchical cluster analysis of DEGs demonstrated a coherent pattern within each group and distinct differences between the groups, confirming the consistency within individual groups and discernible variations across different groups (refer to Fig. S1 and Fig. S2 in the supplemental material).

Enrichment Analysis of DEGs

To gain deeper insights into the biological responses of *T. asahii* to ALA-PDT, we conducted a comprehensive functional enrichment analysis encompassing Gene Ontology (GO) functional categories and Kyoto Encyclopedia of Genes and Genomes (KEGG) pathways. This analysis unveiled the functional implications of both the upregulated and downregulated genes, providing a comprehensive understanding of the molecular events underlying the response of *T. asahii* to ALA-PDT exposure.

Among the identified 2720 DEGs between group $P^{-}L^{-}$ and group $P^{+}L^{100}$, a GOenrichment analysis revealed the top 10 terms with the highest

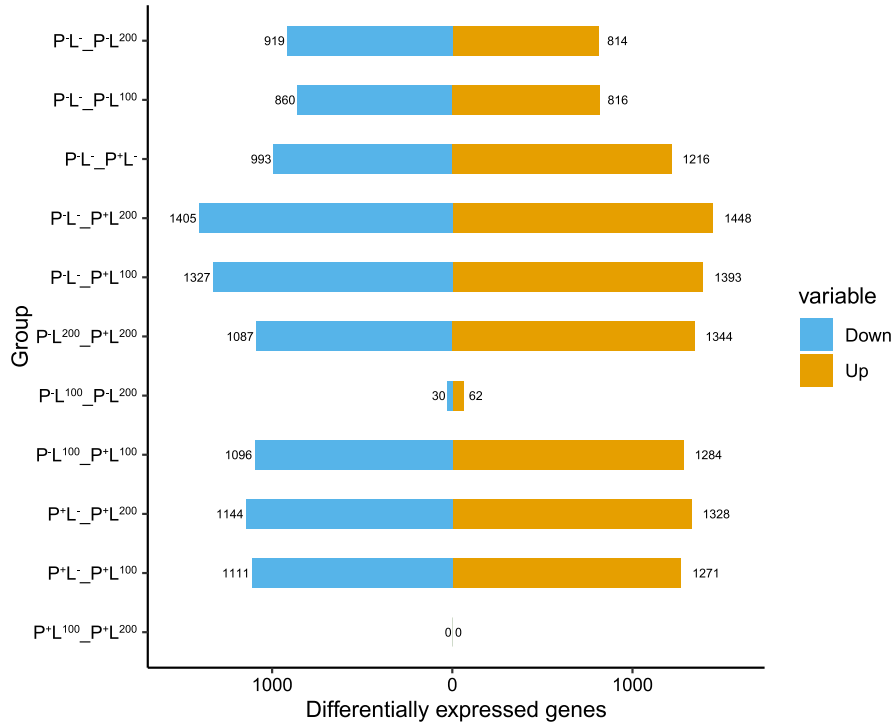

Fig. 3 DEGs Analysis in Various Group Comparisons

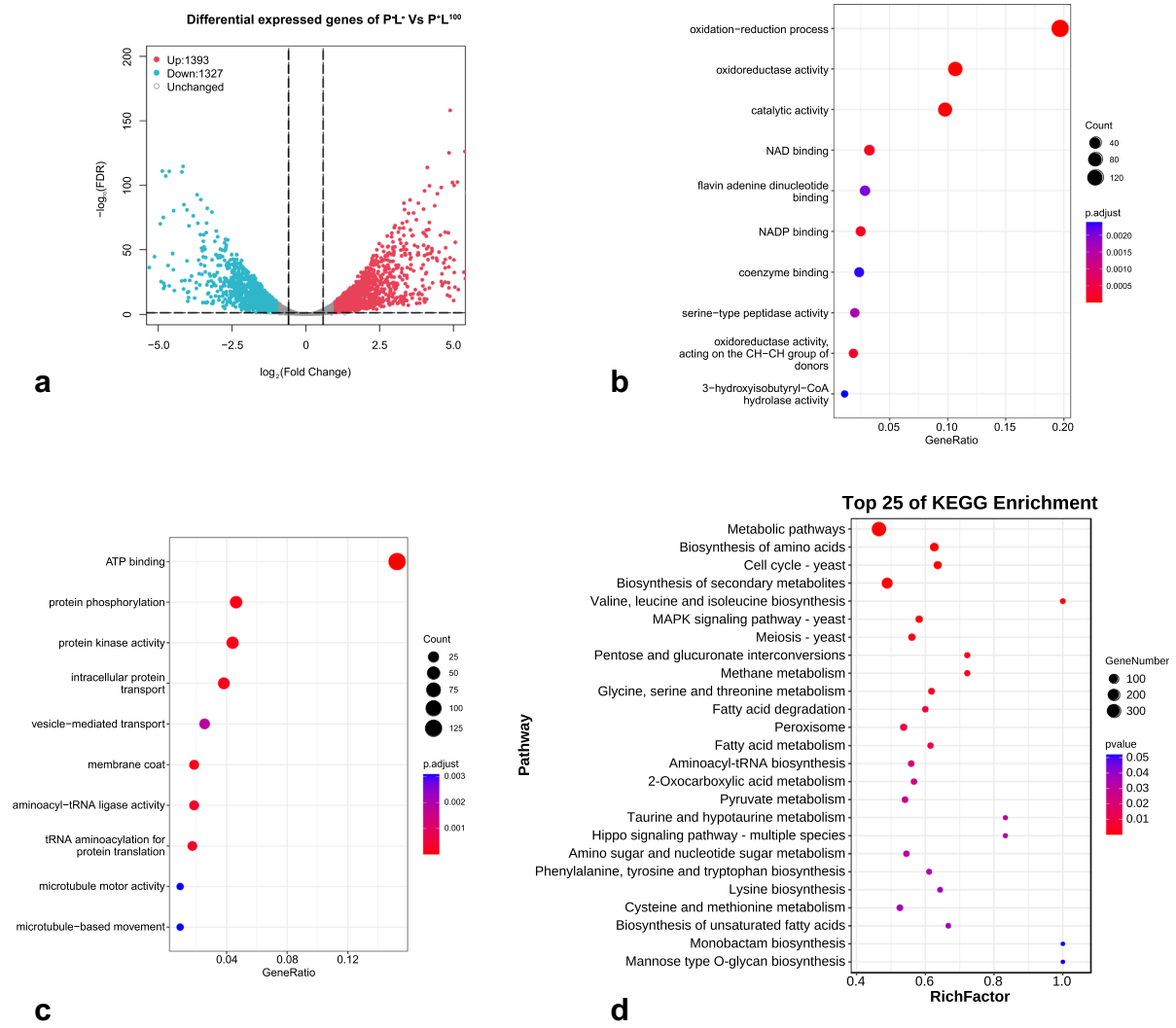

Fig. 4 **a** A Volcano Plot: Differential Expression Analysis Revealed Distinctive Gene Expression Patterns between group $P^{-}L^{-}$ and group $P^{+}L^{100}$ in *T. asahii* biofilms. **b** Top 10 GO terms enriched among the up-regulated DEGs. **c** Top 10 GO terms enriched among the down-regulated DEGs. **d** Top 25 KEGG pathways

representation among the upregulated DEGs. These terms included processes such as oxidation–reduction, oxidoreductase activity, catalytic activity, NAD binding, and coenzyme binding (Fig. 4b). Similarly, the top 10 enriched GO terms among the downregulated DEGs encompassed ATP binding, protein phosphorylation, intracellular protein transport, and microtubule-based movement (Fig. 4c).

Furthermore, KEGG pathway enrichment analysis of 2720 DEGs, with 646 (23.675%) genes annotated, identified the top 25 pathways with the highest representation of DEGs, shedding light on the molecular pathways influenced by ALA-PDT (Fig. 5).

Key DEGs Potentially Involved

In our investigation of key DEGs potentially involved in fungal physiology, we focused on genes associated with important functions such as beta-glucosidase, chitinase, lipase, and ubiquitin. Notably, we observed a downregulation of genes related to sterol biosynthesis, suggesting a potential disruption in the ergosterol biosynthetic pathway.

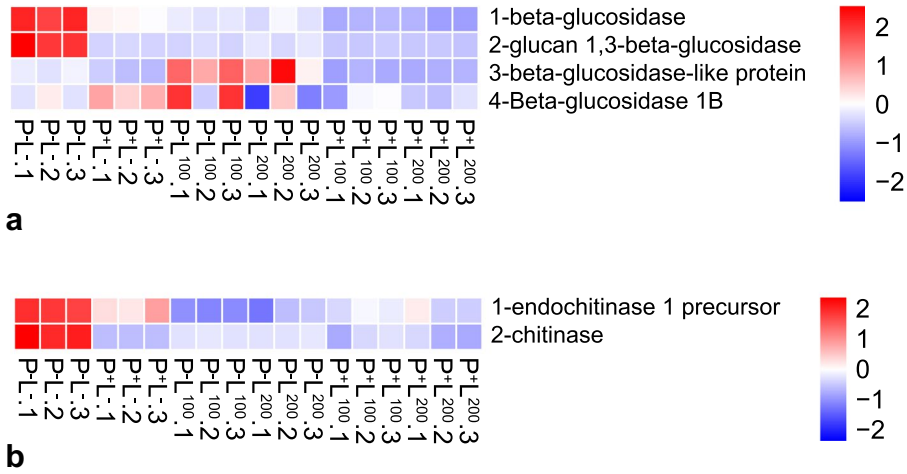

Fig. 5 Genes potentially involved. **a** beta-glucosidase genes; **b** chitinase genes; **c** glucan genes; **d** lipase genes; **e** phospholipase genes; **f** serine genes; **g** sterol genes; **h** ubiquitin genes

Additionally, several genes involved in serine metabolism were downregulated, indicating potential alterations in fungal cellular activity (Fig. 5).

Validation of RNA-Seq by qRT-PCR

We validated the RNA-Seq results through quantitative real-time PCR (qRT-PCR). Our findings revealed a significant increase in the transcriptional levels of the A1Q1_05494 gene, associated with oxidative stress following ALA-PDT treatment. However, no significant difference was observed in the expression of SOD1. Furthermore, ALA-PDT upregulated the transcription of key genes involved in morphogenesis and biofilm formation, namely, A1Q1_04029, A1Q1_01456, A1Q1_01345, and A1Q1_08069. Additionally, an upregulation in the

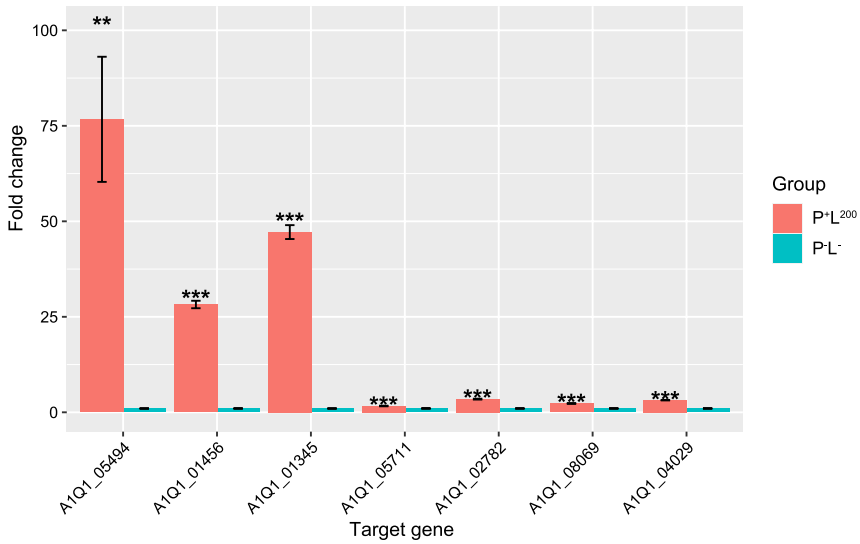

Fig. 6 Quantitative real-time PCR (qRT-PCR) was performed to validate the gene expression levels identified in the RNA-Seq data, specifically for A1Q1_05494, A1Q1_01456, A1Q1_01345, A1Q1_05711, A1Q1_02782, A1Q1_08069, and A1Q1_04029 genes in both the control group (group $P^{-}L^{-}$) and the ALA-PDT group (group $P^{+}L^{100}$). The relative expression levels of differentially expressed genes (DEGs) were represented using a log2 fold change index. The values are presented as the mean ± standard deviation, and statistical significance was indicated as **, or *** for $p < 0.01$ and $p < 0.001$, respectively

transcription of A1Q1_05711 and A1Q1_02782 was also observed (Fig. 6).

Discussion

In the face of mounting resistance to conventional therapeutic modalities, the utilization of PDT has emerged as a promising and compelling treatment strategy, garnering momentum in the battle against persistent and recalcitrant biofilms. PDT is a non-invasive treatment modality that employs photosensitizers, specific-wavelength light, and ROS generation to eliminate undesirable eukaryotic cells or pathogenic microorganisms [29]. ALA is a precursor of the actual photosensitizer protoporphyrin IX (PpIX) in the heme biosynthesis pathway [30]. Unlike conventional photosensitizers, ALA is a commonly used and effective agent in clinical practice. Although it is not intrinsically photodynamically active, irradiation of cells containing ALA generates endogenous PpIX that produces ROS, which constitutes the basic mechanism of PDT-induced cell death [31]. The generated ROS changes the fungal cell wall and membrane, and further transports the photosensitizer into the biofilms, leading to damage to the cell membranes, cytoplasmic organelles, including mitochondria and vacuoles [32, 33].

PDT has exhibited notable efficacy against a diverse array of fungal species, encompassing Candida, Malassezia, Cryptococcus, Dermatophytes, and so on [33]. However, researches on the use of PDT on biofilms are more extensive for Candida compared to other fungi. In a previous in vitro study, ALA-PDT inhibited 74.5% of cells in *C. albicans* biofilms [34]. Afterwards, Greco et al. [35] employed a novel formulation of thermosetting gel ALA in PDT and observed a growth inhibition of approximately 80% in *C. albicans* biofilms. The scientific literature concerning the effects of PDT on *T. asahii* is scarce, with a dearth of previous investigations elucidating the underlying mechanisms of action associated with PDT in this particular species. A previous investigation by Lan et al. [5] exhibited the effectiveness of ALA-PDT against ten strains of *T. asahii* in both the planktonic and biofilm states. The metabolic activities of both types of cells were greatly diminished, with reductions as substantial as 80.8% and 78.9%, respectively, upon exposure to 150 mM and 100 J/cm^2. For the present study, we chose a *T. asahii* strain known for producing robust biofilms. Our findings showcase that ALA-PDT elicits a significant photodynamic response in biofilms of the selected *T. asahii* strain. When subjected to 150 mM and 200 J/cm^2, the metabolic activities of adherent cells was significantly lowered by 75.58% (Fig. 1), as substantiated by CLSM images (Fig. 2). However, when exposed to 150 mM and 100 J/cm^2, the metabolic activities of adherent cells was only reduced by 40%, which was lower than the analogous situation in the previous study and may be attributed to differences in the strain and experimental conditions. Notably, we observed that the inhibition of adherent cells increased with the rise in light density, consistent with the findings of Lan et al. [5]. Furthermore, we determined that neither light nor photosensitizer irradiation alone displayed a lethal effect on *T. asahii*, in agreement with previous literature.

RNA-Seq analysis of the total transcriptome may represent a valuable tool in elucidating the mechanisms underlying the observed antifungal effect exerted by ALA-PDT. Figure 3 depicts the results of the differential gene expression analysis conducted between groups P^+L^{100} and P^+L^{200} following photodynamic treatment of varying durations. Intriguingly, our findings revealed no discernible differential gene expression between these two groups, highlighting the absence of significant transcriptional alterations induced by the duration of photodynamic action between the two groups. However, the greatest number of differential genes was observed between the photodynamic treatment group (P^+L^{100}, P^+L^{200}) and the untreated control group (P^-L^-). It is noteworthy that while the groups exposed to light alone (P^-L^{100}, P^-L^{200}) and the photosensitizer alone group (P^+L^-) did not exhibit a killing effect on *T. asahii* biofilms, they did exert an influence on gene expression. It has been reported that exposure to red light (635 nm) influenced the development and physiology of *C. albicans* biofilms, including their polysaccharide production [36]. A previous report has revealed that the utilization of LED light at 37.5 and 50 J/cm^2 potently induced down-regulation of crucial genes such as ALS1, CAP1, A1Q1_05494, and SOD1, when compared to the control group [37].

As depicted in Fig. 4, GO analysis of up-regulated DEGs in "oxidation–reduction process," "oxidoreductase activity," and "catalytic activity" after ALA-PDT

(group P^-L^- vs. group P^+L^{100}). The effect of PDT promotes the generation of ROS, which subsequently leads to physical damage to the cell membrane [38]. Previous reports found that oxidative stress leads to changes in calcium and lipid metabolism, generating cytokines and stress response mediators that lead to the induction of apoptosis by the mitochondrial pathway and specific protein oxidation [39, 40], which strongly suggest that this intricate mechanism underlies the *T. asahii* death observed in our study. In response to oxidative stress and as a protective mechanism, the fungus can upregulate genes associated with antioxidant activity that assist in safeguarding against free radicals and ROS [41–44]. Therefore, the findings of the present study provide additional evidence that oxidative damage is responsible for the death of *T. asahii* following ALD-PDT treatment.

Down-regulated DEGs were enriched in "ATP binding", "protein phosphorylation" and "protein kinase activity" after ALA-PDT (group P^-L^- vs. group P^+L^{100}). The enrichment of ATP-binding category in GO analysis suggests that genes associated with ATP binding, including those involved in ATP-binding cassette (ABC) transporters, which are a large family of proteins that play a crucial role in the active transport of various molecules across cellular membranes. One of the prominent mechanisms underlying azole tolerance in fungal pathogens involves the upregulation of drug efflux pumps, often belonging to the ABC transporter family. These specific transporters, known as ABCG class transporters, play a crucial role in conferring resistance to azole drugs [45]. In various fungal species, including *Saccharomyces cerevisiae* [46], *C. albicans* [47–49], *Candida glabrata* [50], *Aspergillus fumigatus* [51], *Cryptococcus neoformans* [52], and *Trichophyton rubrum* [53], there is an observed increase in the expression of ABC transporter proteins, which coincides with the development of resistance to azole drugs. This correlation highlights the significance of these transporters in the context of azole resistance across a range of fungal pathogens. The precise involvement of ABC transporters in azole resistance in *T. asahii* is still not fully understood, and further research is needed to clarify their specific role in this context. Our findings revealed a down-regulation in ATP binding, which may provide indirect evidence that photodynamic treatment does not induce increased resistance in *T. asahii*.

Significantly, the investigation uncovered three noteworthy KEGG pathways: "metabolic pathways," "biosynthesis of secondary metabolites," and "cell cycle-yeast," effectively emphasizing the critical role of metabolism, biosynthesis, and cell cycle regulation in the context of photodynamic action. In addition to this, the MAPK pathway was also enriched by KEGG. MAPK pathways represent indispensable sensory mechanisms that translate environmental stimuli into intricate biochemical cascades, ultimately orchestrating adaptive responses to environmental stress [54]. Previously, there are no reports of a MAPK pathway associated with *T. asahii*. Four distinct MAPK pathways have been delineated in *C. albicans*, each encompassing unique functionalities [55, 56]. The cell integrity (PKC) pathway exerts dominion over cell wall biogenesis, morphogenesis, biofilm formation, and virulence. Additionally, the Cek1-mediated pathway orchestrates cell wall construction while governing both mating and the expansive realm of vegetative and invasive growth. Lastly, Cek2, akin to ScFus3, assumes a pivotal role in facilitating optimal mating prowess. Collectively, the present findings underscore the multitude of pathways involved in the realm of photodynamic action against *T. asahii*.

We conducted a further investigation into the key DEGs that may play a role in response to ALA-PDT treatment. The primary sterol in fungi, ergosterol, is a vital constituent of fungal cell membranes, influencing membrane fluidity, permeability, and the function of membrane-associated proteins [57]. Notably, our analysis revealed a down-regulation of genes involved in ergosterol biosynthesis, including lanosterol 14-alpha-demethylase, C-8 sterol isomerase, C-4 methyl sterol oxidase, among others, following ALA-PDT treatment. It is worth mentioning that azole antifungal agents are recognized for their ability to inhibit the synthesis of ergosterol by targeting cytochrome P45014DM, an enzyme that catalyzes the 14α-demethylation of sterols in ergosterol biosynthesis [58]. By disrupting ergosterol production, azoles impair the integrity and functionality of fungal cell membranes, thereby increasing their susceptibility to damage. A previous study by Lan et al. [5] demonstrated that the combination therapy of ALA-PDT with itraconazole resulted in a heightened elimination of both planktonic cells and biofilms, surpassing the effects of the single therapy. Previously, Cláudia Carolina Jordão et al. reported that the expression of

genes related to ergosterol production was significantly reduced by Photodithazine®-PDT [59]. Building upon these findings, we postulate that in addition to ALA-PDT-induced oxidative stress damage, ALA-PDT treatment weakens the biofilm structure, rendering fungal cells more vulnerable to the effects of azole antifungal agents. Our observations provide further insights into the multifaceted mechanisms underlying the synergistic action of ALA-PDT and azole therapy. By targeting ergosterol biosynthesis and biofilm structure, this combination approach exhibits promising potential in enhancing the efficacy of antifungal treatment.

Simultaneously, our investigation revealed a downregulation of DEGs involved in serine metabolism within *T. asahii* biofilms upon ALA-PDT treatment, including serine-tRNA ligase, homoserine kinase, phosphatidylserine decarboxylase 1 (Psd1) precursor, proliferation-associated serine/threonine protein kinase, and serine/threonine-protein phosphatase PP1, when compared to the blank control. The decrease in the expression of these genes may impair protein synthesis and potentially impact crucial cellular functions and growth. Notably, previous research has highlighted the significance of mitochondrial Psd1 in maintaining mitochondrial lipid homeostasis and synthesizing a majority of cellular phosphatidylethanolamine in Saccharomyces cerevisiae, emphasizing its functional role [60]. Additionally, serine/threonine protein kinases, known as pivotal components of diverse signaling pathways in eukaryotes, play critical roles in proliferation and cellular signaling processes [61]. As serine holds prominence as an essential amino acid involved in protein synthesis, phospholipid biosynthesis, and S-adenosylmethionine (SAM) production—a universal methyl donor engaged in epigenetic modifications and gene expression regulation—our inference suggests that genes associated with serine metabolism might serve as important targets for ALA-PDT.

As is illustrated before, production of ROS related to oxidation–reduction process is an important and fundamental mechanism for ALA-PDT and we found up-regulated DEGs in "oxidation–reduction process," "oxidoreductase activity," after ALA-PDT (group $P^{-}L^{-}$ vs. group $P^{+}L^{100}$). As a defense mechanism against oxidative stress, the fungus can express genes associated with antioxidant activity, such as peroxisomal catalase (CAT), and superoxide dismutase (SOD), which play a crucial role in activating pathways that counteract the damaging effects of free radicals and ROS [62, 63]. We further used RNA-Seq to further investigate the mechanisms involved. In the present study, we observed a surge in the transcription of A1Q1_05494 (which may be related to CAT1) (Fig. 6). Jordão et al. [37] found that PDT using Photodithazine® or Curcumin with LED light reduced CAT1 and SOD1 gene expression in *C. albicans* biofilms. In another study by Jordão et al. [59], following Photodithazine® -PDT, CAT1 gene expression was significantly increased in a fluconazole-resistant strain of *C. albicans*. The intricate interplay of photodynamic parameters, encompassing photosensitizer concentration and light intensity [37], alongside distinct temporal stages subsequent to photodynamic treatment [64], may impart a discernible impact on gene transcription. Thus, we posit that our findings diverge from the extant literature not solely owing to interspecies dissimilarities in fungal organisms but rather to a confluence of multifaceted factors.

In our present study, a notable upregulation in the transcriptional activity of key genes associated with morphogenesis and biofilm formation, namely A1Q1_04029 (which may be related to UME6), A1Q1_01456 (which may be related to CPH1), A1Q1_01345 (which may related to EFG1), and A1Q1_08069 (which may related to TEC1), was observed following ALA-PDT treatment in *T. asahii*. In the study conducted by Jing Ma et al. [65], a downregulation in the expression of UME6, EFG1, TEC1, and CPH1 was documented subsequent to curcumin-PDT, suggesting the inhibitory impact of curcumin-PDT on hyphal growth and biofilm formation within *C. albicans* biofilm. In the investigation conducted by Hang Shi et al. [33], it was discovered that ALA-PDT exhibited potent inhibitory effects on *C. albicans* biofilms, accompanied by a consequential downregulation of UME6 gene. In a publication by Freire et al. [66], it was documented that photodynamic inactivation employing either methylene blue or erythrosine as photosensitizers resulted in a reduction in the expression levels of TEC1, CPH1, and EFG1 genes within *C. albicans* biofilms. Previous studies consistently demonstrate the downregulation of UME6, EFG1, TEC1, and CPH1 in response to diverse photodynamic treatments such as curcumin-PDT, ALA-PDT, and PDT utilizing methylene blue or erythrosine as photosensitizers in *C. albicans* biofilms.

These genes bear significant roles in the intricate processes of hyphae formation, morphogenesis, and biofilm development. The marked downregulation of these genes signifies a discernible inhibitory effect on the growth of hyphae and the formation of biofilms. Notably, our current study reveals a noteworthy upregulation in the transcriptional activity of pivotal genes associated with morphogenesis and biofilm formation, specifically A1Q1_04029, A1Q1_01456, A1Q1_01345, and A1Q1_08069, subsequent to ALA-PDT treatment in *T. asahii*. This unexpected response may be attributed to *T. asahii*'s active formation of biofilms as a defensive measure against the damaging effects of ALA-PDT. The specific mechanisms underlying this difference would require further investigation, as different fungal species may have distinct regulatory pathways and gene expression patterns. Besides, specific genes or biological pathways associated with *T. asahii* biofilms have not been extensively verified or characterized in the literature, and research on *T. asahii* biofilms was still relatively limited compared to other fungal species. Since then, we selected the genes in *T. asahii* that showed the highest similarity to those in *C. albicans*. As a result, due to the genomic differences, the functions of these selected genes may not be entirely consistent with those in *C. albicans*. Thus, it is possible that some of these genes may be downregulated in *C. albicans* but upregulated in *T. asahii* due to these differences. Those were the limitations in our research.

In conclusion, our study demonstrates the effective inhibition of *T. asahii* biofilm by ALA-PDT treatment. Moreover, the comprehensive RNA-Seq analysis conducted in this study reveals, for the first time, the transcriptome profile changes in *T. asahii* upon exposure to ALA-PDT. This provides valuable insights into the molecular mechanisms underlying the action of ALA-PDT at the molecular level.

Acknowledgements We are grateful to Peking University First Hospital for kindly offering *T. asahii* isolate 06108. The present investigation benefited from financial backing provided by the National Natural Science Foundation of China (81472892, 81772138), as well as the Beijing Natural Science Foundation, China (7202201). The datasets generated and/or analysed during the current study can be accessed at the China National Center for Bioinformation (accession number PRJCA015533), the NCBI Sequence Read Archive (accession number SRP458245), and the BioProject (accession numberPRJNA1012498).

Author contributions W. L. conducted the majority of experiments and contributed to the initial drafting of the manuscript. G.W. and H.C. conducted partial of the experiments, collected and analyzed the resulting data. G.L. performed partial of the results analysis. W.L. prepared Figs. 1 and Table 1. G.W. and H.C. prepared other figures and tables. The conception of the experiments and the driving of experimental progress were accomplished by the guidance of H.Z. and H.L. All authors reviewed the manuscript. We would like to express our gratitude to Peking University First Hospital for their generous provision of the *T. asahii* isolate 06108.

Funding This work was funded by National Natural Science Foundation of China, 81472892, 81772138, Natural Science Foundation of Beijing Municipality, 7202201.

Declarations

Conflict of interest None.

Ethical Approval The *T. asahii* isolate 06108 used in this study was obtained from a deidentified clinical sample provided by Peking University First Hospital. As the isolate was not linked to any patient-identifiable information, this work does not fall under the requirement for specific ethical approval according to institutional guidelines. Nevertheless, the study adhered to the Declaration of Helsinki principles and institutional ethical standards.

References

1. Colombo AL, Padovan AC, Chaves GM. Current knowledge of *Trichosporon* spp. and Trichosporonosis. Clin Microbiol Rev. 2011;24:682–700. https://doi.org/10.1128/CMR.00003-11.
2. Guo LN, et al. Invasive infections due to *Trichosporon*: species distribution genotyping, and antifungal susceptibilities from a multicenter study in China. J Clin Microbiol. 2019. https://doi.org/10.1128/JCM.01505-18.

3. Ramírez I, Moncada D. Fatal disseminated infection by *Trichosporon asahii* under voriconazole therapy in a patient with Acute Myeloid Leukemia: a review of breakthrough infections by *Trichosporon* spp. Mycopathologia. 2020;185:377–88. https://doi.org/10.1007/s11046-019-00416-w.
4. de Almeida Junior JN, Hennequin C. Invasive *Trichosporon* infection: a systematic review on a re-emerging fungal pathogen. Front Microbiol. 2016;7:1629. https://doi.org/10.3389/fmicb.2016.01629.
5. Lan Y, et al. Combinatory effect of ALA-PDT and itraconazole treatment for *Trichosporon asahii*. Lasers Surg Med. 2020. https://doi.org/10.1002/lsm.23343.
6. Wolf DG, et al. Multidrug-resistant *Trichosporon asahii* infection of nongranulocytopenic patients in three intensive care units. J Clin Microbiol. 2001;39:4420–5. https://doi.org/10.1128/JCM.39.12.4420-4425.2001.
7. Biasoli MS, et al. Systemic infection caused by *Trichosporon asahii* in a patient with liver transplant. Med Mycol. 2008;46:719–23. https://doi.org/10.1080/13693780802232928.
8. Gross JW, Kan VL. *Trichosporon asahii* infection in an advanced AIDS patient and literature review. AIDS. 2008;22:793–5. https://doi.org/10.1097/QAD.0b013e3282f51ecc.
9. Bayramoglu G, Sonmez M, Tosun I, Aydin K, Aydin F. Breakthrough *Trichosporon asahii* fungemia in neutropenic patient with acute leukemia while receiving caspofungin. Infection. 2008;36:68–70. https://doi.org/10.1007/s15010-007-6278-6.
10. Kim SH, et al. Chronic cutaneous disseminated *Trichosporon asahii* infection in a nonimmunocompromised patient. J Am Acad Dermatol. 2008;59:S37-39. https://doi.org/10.1016/j.jaad.2007.08.017.
11. Rastogi VL, Nirwan PS. Invasive trichosporonosis due to *Trichosporon asahii* in a non-immunocompromised host: a rare case report. Indian J Med Microbiol. 2007;25:59–61. https://doi.org/10.4103/0255-0857.31065.
12 Nobrega de Almeida J, et al. *Trichosporon asahii* superinfections in critically ill COVID-19 patients overexposed to antimicrobials and corticosteroids. Mycoses. 2021;64:817–22. https://doi.org/10.1111/myc.13333.
13. Iturrieta-Gonzalez IA, Padovan AC, Bizerra FC, Hahn RC, Colombo AL. Multiple species of *Trichosporon* produce biofilms highly resistant to triazoles and amphotericin B. PLoS ONE. 2014. https://doi.org/10.1371/journal.pone.0109553.
14. Fuentefria AM, Pippi B, Dalla Lana DF, Donato KK, de Andrade SF. Antifungals discovery: an insight into new strategies to combat antifungal resistance. Lett Appl Microbiol. 2018;66:2–13. https://doi.org/10.1111/lam.12820.
15. Pierce CG, Srinivasan A, Uppuluri P, Ramasubramanian AK, Lopez-Ribot JL. Antifungal therapy with an emphasis on biofilms. Curr Opin Pharmacol. 2013;13:726–30. https://doi.org/10.1016/j.coph.2013.08.008.
16. Jori G, et al. Photodynamic therapy in the treatment of microbial infections: basic principles and perspective applications. Lasers Surg Med. 2006;38:468–81. https://doi.org/10.1002/lsm.20361.
17. Wainwright M, et al. Photoantimicrobials-are we afraid of the light? Lancet Infect Dis. 2017;17:e49–55. https://doi.org/10.1016/S1473-3099(16)30268-7.
18. Hamblin MR, Hasan T. Photodynamic therapy: a new antimicrobial approach to infectious disease? Photochem Photobiol Sci. 2004;3:436–50. https://doi.org/10.1039/b311900a.
19. Dai T, et al. Concepts and principles of photodynamic therapy as an alternative antifungal discovery platform. Front Microbiol. 2012;3:120. https://doi.org/10.3389/fmicb.2012.00120.
20. Donnelly RF, McCarron PA, Tunney MM. Antifungal photodynamic therapy. Microbiol Res. 2008;163:1–12. https://doi.org/10.1016/j.micres.2007.08.001.
21. Lee JW, Kim BJ, Kim MN. Photodynamic therapy: new treatment for recalcitrant Malassezia folliculitis. Lasers Surg Med. 2010;42:192–6. https://doi.org/10.1002/lsm.20857.
22. Sotiriou E, Panagiotidou D, Ioannides D. 5-Aminolevulinic acid photodynamic therapy treatment for tinea cruris caused by *Trichophyton rubrum*: report of 10 cases. J Eur Acad Dermatol Venereol. 2009;23:341–2. https://doi.org/10.1111/j.1468-3083.2008.02880.x.
23. Kim D, Langmead B, Salzberg SL. HISAT: a fast spliced aligner with low memory requirements. Nat Methods. 2015;12:357–60. https://doi.org/10.1038/nmeth.3317.
24. Pertea M, et al. StringTie enables improved reconstruction of a transcriptome from RNA-seq reads. Nat Biotechnol. 2015;33:290–5. https://doi.org/10.1038/nbt.3122.
25. Pertea M, Kim D, Pertea GM, Leek JT, Salzberg SL. Transcript-level expression analysis of RNA-seq experiments with HISAT. StringTie and Ballgown Nat Protoc. 2016;11:1650–67. https://doi.org/10.1038/nprot.2016.095.
26. Love MI, Huber W, Anders S. Moderated estimation of fold change and dispersion for RNA-seq data with DESeq2. Genome Biol. 2014;15:550. https://doi.org/10.1186/s13059-014-0550-8.
27. Chen T, et al. The genome sequence archive family: toward explosive data growth and diverse data types. Genom Proteom Bioinf. 2021;19:578–83. https://doi.org/10.1016/j.gpb.2021.08.001.
28. Members C-N, et al. Database resources of the national genomics data center, china national center for bioinformation in 2022. Nucleic Acids Res. 2022;50:D27–38. https://doi.org/10.1093/nar/gkab951.
29 Stajer A, Kajari S, Gajdacs M, Musah-Eroje A, Barath Z. Utility of photodynamic therapy in dentistry: current concepts. Dent J (Basel). 2020. https://doi.org/10.3390/dj8020043.
30. Krammer B, Plaetzer K. ALA and its clinical impact, from bench to bedside. Photochem Photobiol Sci. 2008;7:283–9. https://doi.org/10.1039/b712847a.
31. Harris F, Pierpoint L. Photodynamic therapy based on 5-aminolevulinic acid and its use as an antimicrobial agent. Med Res Rev. 2012;32:1292–327. https://doi.org/10.1002/med.20251.
32. Baltazar LM, et al. Antimicrobial photodynamic therapy: an effective alternative approach to control fungal infections. Front Microbiol. 2015;6:202. https://doi.org/10.3389/fmicb.2015.00202.

33. Shi H, Li J, Peng C, Xu B, Sun H. The inhibitory activity of 5-aminolevulinic acid photodynamic therapy (ALA-PDT) on Candida albicans biofilms. Photodiagnosis Photodyn Ther. 2021;34:102271. https://doi.org/10.1016/j.pdpdt.2021.102271.
34. Shi H, Li J, Zhang H, Zhang J, Sun H. Effect of 5-aminolevulinic acid photodynamic therapy on Candida albicans biofilms: an in vitro study. Photodiagnosis Photodyn Ther. 2016;15:40–5. https://doi.org/10.1016/j.pdpdt.2016.04.011.
35. Greco G, et al. Newly formulated 5% 5-aminolevulinic acid photodynamic therapy on Candida albicans. Photodiagnosis Photodyn Ther. 2020;29:101575. https://doi.org/10.1016/j.pdpdt.2019.10.010.
36. da Silveira PV, et al. Twice-daily red and blue light treatment for Candida albicans biofilm matrix development control. Lasers Med Sci. 2019;34:441–7. https://doi.org/10.1007/s10103-018-2610-x.
37. Jordao CC, et al. Antimicrobial photodynamic therapy reduces gene expression of Candida albicans in biofilms. Photodiagnosis Photodyn Ther. 2020;31:101825. https://doi.org/10.1016/j.pdpdt.2020.101825.
38. Cuadrado CF, et al. Broad-spectrum antimicrobial ZnMintPc encapsulated in magnetic-nanocomposites with graphene oxide/MWCNTs Based on bimodal action of photodynamic and photothermal effects. Pharmaceutics. 2022. https://doi.org/10.3390/pharmaceutics14040705.
39. Lang W, Lang M, Goldenberg G, Podreka I, Deecke L. EEG and rCBF evidence for left frontocortical activation when memorizing verbal material. Electroencephalogr Clin Neurophysiol Suppl. 1987;40:328–34.
40. Mroz P, Yaroslavsky A, Kharkwal GB, Hamblin MR. Cell death pathways in photodynamic therapy of cancer. Cancers (Basel). 2011;3:2516–39. https://doi.org/10.3390/cancers3022516.
41 Dantas Ada S, et al. Oxidative stress responses in the human fungal pathogen, *Candida* albicans. Biomolecules. 2015;5:142–65. https://doi.org/10.3390/biom5010142.
42. Wysong DR, Christin L, Sugar AM, Robbins PW, Diamond RD. Cloning and sequencing of a *Candida* albicans catalase gene and effects of disruption of this gene. Infect Immun. 1998;66:1953–61. https://doi.org/10.1128/IAI.66.5.1953-1961.1998.
43. Martchenko M, Alarco AM, Harcus D, Whiteway M. Superoxide dismutases in *Candida* albicans: transcriptional regulation and functional characterization of the hyphal-induced SOD5 gene. Mol Biol Cell. 2004;15:456–67. https://doi.org/10.1091/mbc.e03-03-0179.
44. Enjalbert B, et al. Role of the Hog1 stress-activated protein kinase in the global transcriptional response to stress in the fungal pathogen *Candida* albicans. Mol Biol Cell. 2006;17:1018–32. https://doi.org/10.1091/mbc.e05-06-0501.
45. Gulshan K, Moye-Rowley WS. Multidrug resistance in fungi. Eukaryot Cell. 2007;6:1933–42. https://doi.org/10.1128/EC.00254-07.
46. Shahi P, Moye-Rowley WS. Coordinate control of lipid composition and drug transport activities is required for normal multidrug resistance in fungi. Biochim Biophys Acta. 2009;1794:852–9. https://doi.org/10.1016/j.bbapap.2008.12.012.
47. Prasad R, De Wergifosse P, Goffeau A, Balzi E. Molecular cloning and characterization of a novel gene of *Candida* albicans, CDR1, conferring multiple resistance to drugs and antifungals. Curr Genet. 1995;27:320–9. https://doi.org/10.1007/BF00352101.
48. Sanglard D, et al. Mechanisms of resistance to azole antifungal agents in *Candida* albicans isolates from AIDS patients involve specific multidrug transporters. Antimicrob Agents Chemother. 1995;39:2378–86. https://doi.org/10.1128/AAC.39.11.2378.
49. Ren B, et al. ABC transporters coupled with the elevated ergosterol contents contribute to the azole resistance and amphotericin B susceptibility. Appl Microbiol Biotechnol. 2014;98:2609–16. https://doi.org/10.1007/s00253-013-5425-5.
50. Miyazaki H, et al. Fluconazole resistance associated with drug efflux and increased transcription of a drug transporter gene, PDH1 *Candida* glabrata. Antimicrob Agents Chemother. 1998;42:1695–701. https://doi.org/10.1128/AAC.42.7.1695.
51. Paul S, Diekema D, Moye-Rowley WS. Contributions of *Aspergillus fumigatus* ATP-binding cassette transporter proteins to drug resistance and virulence. Eukaryot Cell. 2013;12:1619–28. https://doi.org/10.1128/EC.00171-13.
52 Oliveira NK, Bhattacharya S, Gambhir R, Joshi M, Fries BC. Novel ABC transporter associated with Fluconazole resistance in aging of *Cryptococcus* neoformans. J Fungi (Basel). 2022. https://doi.org/10.3390/jof8070677.
53. Monod M, et al. *Trichophyton rubrum* azole resistance mediated by a new ABC transporter, TruMDR3. Antimicrob Agents Chemother. 2019. https://doi.org/10.1128/AAC.00863-19.
54. Roman E, Correia I, Prieto D, Alonso R, Pla J. The HOG MAPK pathway in *Candida* albicans: more than an osmosensing pathway. Int Microbiol. 2020;23:23–9. https://doi.org/10.1007/s10123-019-00069-1.
55. Monge RA, Roman E, Nombela C, Pla J. The MAP kinase signal transduction network in *Candida* albicans. Microbiology (Reading). 2006;152:905–12. https://doi.org/10.1099/mic.0.28616-0.
56. Roman E, Arana DM, Nombela C, Alonso-Monge R, Pla J. MAP kinase pathways as regulators of fungal virulence. Trends Microbiol. 2007;15:181–90. https://doi.org/10.1016/j.tim.2007.02.001.
57 Jorda T, Puig S. Regulation of ergosterol biosynthesis in *Saccharomyces cerevisiae*. Genes (Basel). 2020. https://doi.org/10.3390/genes11070795.
58 van den Bossche H, Willemsens G, Cools W, Lauwers WF, Le Jeune L. Biochemical effects of miconazole on fungi. II. Inhibition of ergosterol biosynthesis in *Candida* albicans. Chem Biol Interact. 1978;21:59–78. https://doi.org/10.1016/0009-2797(78)90068-6.
59. Jordao CC, Klein MI, Carmello JC, Dias LM, Pavarina AC. Consecutive treatments with photodynamic therapy and nystatin altered the expression of virulence and ergosterol biosynthesis genes of a fluconazole-resistant *Candida* albicans in vivo. Photodiagnosis Photodyn Ther. 2021;33:102155. https://doi.org/10.1016/j.pdpdt.2020.102155.
60. Horvath SE, et al. Processing and topology of the yeast mitochondrial phosphatidylserine decarboxylase 1. J Biol

Chem. 2012;287:36744–55. https://doi.org/10.1074/jbc.M112.398107.
61. Ben-Sahra I, Manning BD. mTORC1 signaling and the metabolic control of cell growth. Curr Opin Cell Biol. 2017;45:72–82. https://doi.org/10.1016/j.ceb.2017.02.012.
62. Westwater C, Balish E, Schofield DA. Candida albicans-conditioned medium protects yeast cells from oxidative stress: a possible link between quorum sensing and oxidative stress resistance. Eukaryot Cell. 2005;4:1654–61. https://doi.org/10.1128/EC.4.10.1654-1661.2005.
63. Abad A, et al. What makes *Aspergillus fumigatus* a successful pathogen? Genes and molecules involved in invasive aspergillosis. Rev Iberoam Micol. 2010;27:155–82. https://doi.org/10.1016/j.riam.2010.10.003.
64. Alonso GC, Klein MI, Jordao CC, Carmello JC, Pavarina AC. Gene expression of *Candida* albicans strains isolates from patients with denture stomatitis submitted to treatments with photodynamic therapy and nystatin. Photodiagnosis Photodyn Ther. 2021;35:102292. https://doi.org/10.1016/j.pdpdt.2021.102292.
65. Ma J, Shi H, Sun H, Li J, Bai Y. Antifungal effect of photodynamic therapy mediated by curcumin on *Candida* albicans biofilms in vitro. Photodiagnosis Photodyn Ther. 2019;27:280–7. https://doi.org/10.1016/j.pdpdt.2019.06.015.
66. Freire F, de Barros PP, Pereira CA, Junqueira JC, Jorge AOC. Photodynamic inactivation in the expression of the *Candida* albicans genes ALS3, HWP1, BCR1, TEC1, CPH1, and EFG1 in biofilms. Lasers Med Sci. 2018;33:1447–54. https://doi.org/10.1007/s10103-018-2487-8.